CrystEngComm

Cite this: *CrystEngComm*, 2012, **14**, 2748

www.rsc.org/crystengcomm

PAPER

Guest-dependent host structures and host-induced guest assemblies†

Hye Jeong Park and Myunghyun Paik Suh*

Received 11th August 2011, Accepted 22nd December 2011
DOI: 10.1039/c2ce06040j

Coordination polymer networks, $[Cu_2(C_{26}H_{52}N_{10})(BDC)_2]\cdot 4H_2O$ (**1**) and $[Cu_2(C_{26}H_{52}N_{10})(BDC)_2]\cdot 2DHB\cdot 4H_2O$ (**2**) with 2D brick-wall structures, $[Cu_2(C_{26}H_{52}N_{10})(BDC)_2]\cdot 4HB\cdot 4H_2O$ (**3**) with a 1D ladder structure, and $[Cu_2(C_{26}H_{52}N_{10})(BDC)(H_2O)_2]\cdot 2$(THB)-(BDC)$\cdot 8H_2O$ (**4**) with a 1D chain structure, have been assembled in water from a Cu^{II} bismacrocyclic complex $[Cu_2(C_{26}H_{52}N_{10})(Cl)_4]\cdot 6H_2O$ (**A**) and sodium 1,4-benzenedicarboxylate (Na_2BDC) in the presence of no organic guest for **1**, 1,4-dihydroxybenzene (DHB) for **2**, hydroxybenzene (HB) for **3**, and 1,3,5-trihydroxybenzene (THB) for **4**. In the assembly of the networks, the guest molecule acts as a template and stabilizes the host structure by the hydrogen bonding or π–π stacking interactions. In addition, the guest molecules interact with each other as well as with the host to form 1D columns that occupy the channels in **1**, **2**, and **3**, and the 2D noncovalent organic layers that are alternately packed with the host layers in **4**.

Introduction

Functional coordination polymer networks (CPNs) can be prepared by selecting proper metal and organic building blocks based on crystal engineering. In particular, they can be assembled to generate cavities or channels of various sizes and shapes, which have potential applications in molecular adsorption and separation processes,[1–6] ion-exchange,[7] fabrication of metal nanoparticles,[3a,8] and sensor technology.[9] In CPNs, the pores and channels are filled with guest molecules which interact with the host framework *via* hydrogen bonding, π–π stacking interactions, or CH–π interactions.[3a,10] Combination of these weak interactions in the CPNs induces flexible and dynamic nature of the networks that respond to external stimuli.[11] A considerable number of studies have been conducted on the effect of the guest exchange on the framework structure.[10] The type of guest molecule must play a crucial role to determine the host structure by acting as a template in the self-assembly of CPNs. However, there have been a few reports revealing how the template guest molecules affect the host framework structure.[12]

For the design and assembly of CPNs, free metal ions are commonly used as the metal building blocks, and macrocyclic complexes have seldom been employed. However, square planar macrocyclic complexes can be employed as useful metal building blocks since they act as linear linkers for the organic ligand, which makes design and assembly of the network simple and easy.[1–3] Especially, a bismacrocyclic complex containing two metal ions is a useful metal building block because both metal ions are involved in coordinating the organic ligand and inducing the formation of multidimensional networks.[1] In addition, the flexibility and functionality of CPNs can be varied by changing the bridging unit of the bismacrocyclic complex.[1,2] The Cu^{II} macrocyclic complexes belong to rather unexplored class of building blocks[3c] because of the Jahn–Teller effect of the Cu^{II} ion, which induces weak binding with the ligand at the axial position.

Here, we report various coordination polymers, $[Cu_2(C_{26}H_{52}N_{10})(BDC)_2]\cdot 4H_2O$ (**1**), $[Cu_2(C_{26}H_{52}N_{10})(BDC)_2]\cdot 2$(1,4-dihydroxybenzene)$\cdot 4H_2O$ (**2**), $[Cu_2(C_{26}H_{52}N_{10})(BDC)_2]\cdot 4$(hydroxybenzene)$\cdot 4H_2O$ (**3**), and $[Cu_2(C_{26}H_{52}N_{10})(BDC)(H_2O)_2]\cdot 2$(1,3,5-trihydroxybenzene)-(BDC)$\cdot 8H_2O$ (**4**), which have been self-assembled in water from a Cu^{II} bismacrocyclic complex, $[Cu_2(C_{26}H_{52}N_{10})(Cl)_4]\cdot 6H_2O$ (**A**), and sodium 1,4-benzenedicarboxylate (Na_2BDC) in the presence of various phenol type guest molecules. In the self-assembly, the guest molecules play a crucial role in determining the host structures. The guest molecules also form various networks by the intermolecular hydrogen bonding and π–π stacking interactions, which are again affected by the host networks and included in the host. The resulting networks are shown schematically in Scheme 1. The crystallographic data of **1–4** are summarized in Table 1. The crystal structures are compared in Table 2.

Results and discussion

Properties and X-ray crystal structure of $[Cu_2(C_{26}H_{52}N_{10})(BDC)_2]\cdot 4H_2O$ (1)

The Cu^{II} bismacrocyclic complex (**A**) was prepared as a metal building block eqn (1) by modifying the one-pot metal–template condensation reactions that we previously developed.[2,13,14]

Department of Chemistry, Seoul National University, Seoul, 151-747, Republic of Korea. E-mail: mpsuh@snu.ac.kr; Fax: +82-2-886-8516; Tel: +82-2-880-7760

† Electronic supplementary information (ESI) available: TGA/DSC traces for **1–4**. CCDC reference numbers 747625 (**1**), 747626 (**2**), 747627 (**3**), and 747628 (**4**). For ESI and crystallographic data in CIF or other electronic format see DOI: 10.1039/c2ce06040j/

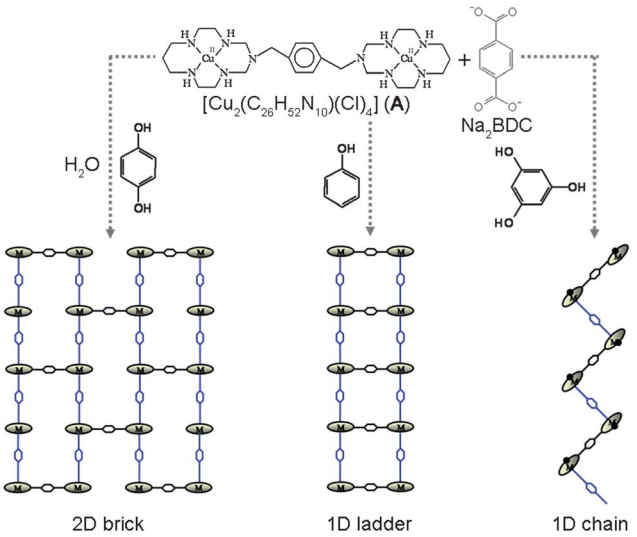

Scheme 1 Self-assembly of **A** and Na_2BDC in the presence of water and various phenol type guest molecules.

$$CuCl_2 + H_2N(CH_2)_2HN(CH_2)_3NH(CH_2)_2NH_2 + CH_2O + p\text{-}C_6H_4(CH_2NH_2)_2 \rightarrow \mathbf{A} \quad (1)$$

By mixing an aqueous solution of **A** and an aqueous solution of sodium 1,4-benzenedicarboxylate (Na_2BDC), a puckered 2D layer with the brick-wall motif was assembled. The solid **1** is soluble in water but insoluble in common organic solvents such as MeCN, MeOH, DMF, $CHCl_3$, THF, toluene, hexane, and acetone. The ORTEP drawing of the fundamental building unit of **1** is shown in Fig. 1a. An inversion centre is located at the centroid of the xylyl group of the bismacrocyclic complex. In **1**, each Cu^{II} ion is coordinated with two BDC^{2-} ions at the apical positions and each BDC^{2-} ion binds two Cu^{II} macrocyclic units (Fig. 1b). The Cu^{II} ions show strong Jahn–Teller distortion, having the average Cu–O(BDC^{2-}) bond distance of 2.710(2) Å and the average Cu–N(macrocycle) bond distance of 2.012(2) Å. The coordination of Cu^{II} and BDC^{2-} is reinforced by the intramolecular hydrogen bonds between the uncoordinated carbonyl oxygen atom of BDC^{2-} and the *sec*-amines of macrocycle to form a stable six-membered ring (Table 3). Each cavity in the 2D layer is formed of four BDC^{2-} units and six Cu^{II} ions. The 2D layers extend parallel to the $(20\bar{1})$ plane and they are stacked in the

Table 2 Comparison of average Cu–O(axial), Cu–N(macrocycle) bond distances (Å), and diffuse reflectance UV/Vis spectra (λ_{max}) of **1–4**

Compound	1	2	3	4
Av. Cu–O/Å	2.710(2)	2.415(4)	2.395(2)	2.642(2)
Av. Cu–N/Å	2.012(2)	2.020(3)	2.014(2)	2.008(2)
λ_{max}/nm	514	540	543	505

Table 1 Crystallographic data of **1–4**

	1	2	3	4
Formula	$Cu_2C_{42}H_{68}N_{10}O_{12}$	$Cu_2C_{54}H_{80}N_{10}O_{16}$	$Cu_2C_{66}H_{92}N_{10}O_{16}$	$Cu_2C_{54}H_{92}N_{10}O_{24}$
Crystal system	Monoclinic	Monoclinic	Triclinic	Monoclinic
Space group	$P2_1/c$	$P2_1/c$	$P\bar{1}$	$P2_1/c$
fw	1032.14	1252.36	1408.58	1392.46
a/Å	7.8814(4)	11.0014(4)	10.4604(5)	16.5171(3)
b/Å	16.4329(13)	16.1868(6)	11.9640(7)	11.3860(3)
c/Å	18.0521(13)	17.8272(7)	16.1087(8)	17.9517(5)
α/deg	90	90	78.673(3)	90
β/deg	90.406(4)	106.526(2)	72.493(3)	106.933(1)
γ/deg	90	90	64.513(3)	90
V/Å^3	2337.9(3)	3043.5(2)	1730.2(2)	3229.7(1)
Z	2	2	1	2
ρ_{calcd}/g cm^{-3}	1.466	1.367	1.352	1.432
Temp/K	293(2)	293(2)	293(2)	293(2)
λ/Å	0.71073	0.71073	0.71073	0.71073
μ/mm^{-1}	0.981	0.772	0.687	0.744
GOF (F^2)	1.060	1.099	1.101	1.075
F(000)	1088	1320	744	1472
Reflections collected	8869	11 902	11 371	13 636
Independent reflections	5210 [R(int) = 0.0575]	6490 [R(int) = 0.1264]	7888 [R(int) = 0.0321]	7276 [R(int) = 0.0691]
Completeness to θ_{max} (%)	96.8	95.1	98.9	98.9
Data/parameters/restraints	5210/298/0	6490/372/0	7888/426/0	7276/409/0
θ Range for data collection/deg	1.68–27.50	1.73–27.26	1.33–27.52	1.29–27.41
Diffraction limits/h, k, l	$-10 \le h \le 10$, $-21 \le k \le 20$, $-23 \le l \le 23$	$-14 \le h \le 14$, $-20 \le k \le 20$, $-22 \le l \le 22$	$-12 \le h \le 13$, $-15 \le k \le 15$, $-20 \le l \le 20$	$-21 \le h \le 21$, $-14 \le k \le 14$, $-23 \le l \le 23$
Refinement method	Full-matrix least-squares on F^2	Full-matrix least-squares on F^2	Full-matrix least-squares on F^2	Full-matrix least-squares on F^2
$R_1{}^a$, w$R_2{}^b$ [$I > 2\sigma(I)$]	0.0639, 0.1664	0.0884, 0.2230	0.0616, 0.1748	0.0695, 0.1888
$R_1{}^a$, w$R_2{}^b$ (all data)	0.1067, 0.2061	0.2395, 0.3108	0.1203, 0.2233	0.1473, 0.2434
Largest peak, hole/e Å^{-3}	0.573, −1.240	0.811, −1.199	0.907, −1.091	0.763, −1.034

[a] $R_1 = \Sigma||F_0| - |F_C||/\Sigma|F_0|$. [b] $wR_2(F^2) = [\Sigma w(F_0^2 - F_C^2)^2/\Sigma w(F_0^2)^2]^{1/2}$ where $w = 1/[\sigma^2(F_0^2) + (0.1243P)^2 + 0.00P]$, $P = (F_0^2 + 2F_C^2)/3$ for **1**, $w = 1/[\sigma^2(F_0^2) + (0.1434P)^2 + 2.27P]$, $P = (F_0^2 + 2F_C^2)/3$ for **2**, $w = 1/[\sigma^2(F_0^2) + (0.1225P)^2 + 0.00P]$, $P = (F_0^2 + 2F_C^2)/3$ for **3**, and $w = 1/[\sigma^2(F_0^2) + (0.1318P)^2 + 0.96P]$, $P = (F_0^2 + 2F_C^2)/3$ for **4**.

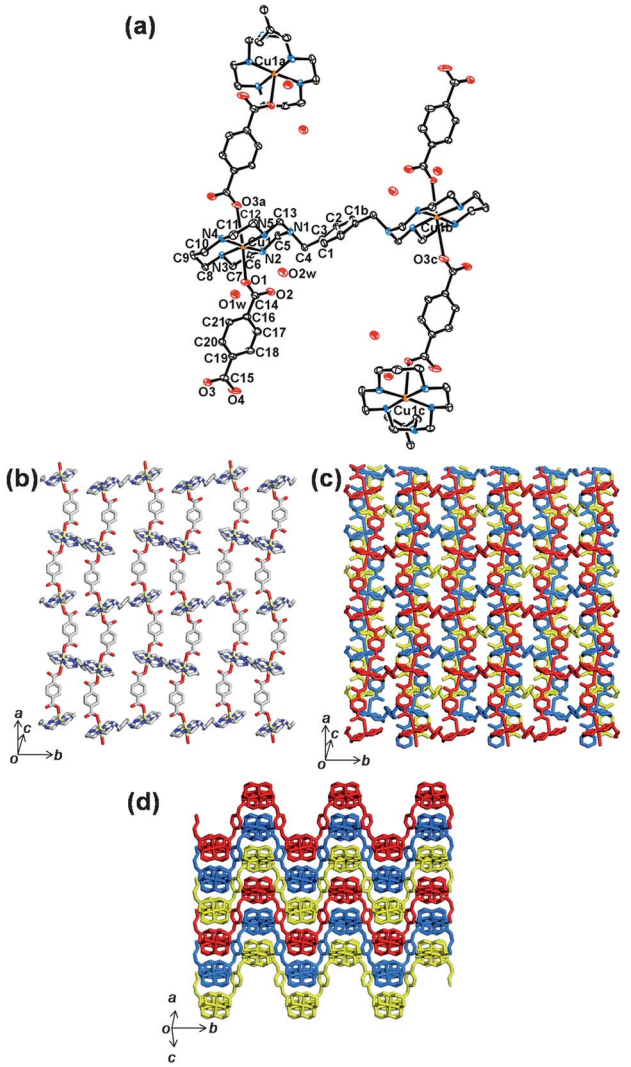

Fig. 1 The X-ray crystal structure of **1**. (a) An ORTEP drawing with the atomic numbering scheme. The atoms are represented by 30% probable thermal ellipsoids. Symmetry operations: *a* ($x - 1, -y + 1/2, z - 1/2$), *b* ($-x + 1, -y, -z$), and *c* ($-x + 2, y - 1/2, -z + 1/2$). (b) Top view of the 2D layer of **1** showing the brick-wall motif. (c) The stacking mode of the 2D layers in **1**. The guest water molecules are omitted for clarity. (d) Side view of **1**, the puckered 2D layers in **1** are closely packed by fitting the grooves together.

ABCABC… manner with a slipped style so that the cavity with 21.8×11.4 Å^2 cross-section (effective void size, 18.4×8.0 Å^2) is divided into three smaller rectangles (Fig. 1c and d). The shortest Cu···Cu distance between two adjacent layers is 7.881(0) Å. The cavities are occupied by water guest molecules, which are hydrogen bonded with uncoordinated carbonyl oxygen atom of BDC^{2-} as well as with *sec*-amine nitrogen of the macrocycle in the host (Table 3). However, they do not interact with each other (the shortest distance between two adjacent water guest molecules is 3.551(5) Å).

The void volume without the guest water molecules in a unit cell is estimated as 97.7 Å^3 (4.2%) by PLATON.[15] Thermogravimetric analysis (TGA) data for the crystalline sample **1** indicate 6.7% weight loss at 40–95 °C, corresponding to the loss of four water guest molecules (calcd, 7.0%) per formula unit. No further weight loss was observed up to 245 °C (Fig. S1†). In spite of the structural stability of apohost, the gas sorption study on the dried solid gave a Langmuir surface area of only 21.5 m^2 g^{-1} (DR micropore volume, 0.00317 cm^3 g^{-1}), indicating its poor porosity.[16] Because the puckered 2D layers in **1** are closely packed by fitting the grooves formed by the planar ligands with the macrocyclic species together, open channel or space is hardly created between the layers.

Properties and X-ray crystal structure of $[Cu_2(C_{26}H_{52}N_{10})(BDC)_2]\cdot 2DHB\cdot 4H_2O$ (2)

By mixing an aqueous solution of Cu^{II} bismacrocyclic complex of **A** and sodium 1,4-benzenedicarboxylate (Na_2BDC) in the presence of 1,4-dihydroxybenzene (DHB), a 2D layer with brick-wall motif was assembled, similar to that of **1**. The solid **2** is soluble in water but insoluble in common organic solvents such as MeCN, MeOH, DMF, $CHCl_3$, THF, toluene, hexane, and acetone. The ORTEP drawing of **2** is shown in Fig. 2a. The bismacrocyclic complex and two guest DHB moieties lie about independent inversion centres in the unit cell: (1/2, 1/2, 1/2), (0, 1/2, 0), and (1/2, 1/2, 0), respectively. Each cavity in the 2D layer is formed by four BDC^{2-} units and six Cu^{II} ions (Fig. 2b). It has rectangular cavities with edge lengths of 23.2×12.0 Å^2 with an effective void size of 19.8×8.6 Å^2, in which DHB molecules are included *via* π–π interactions with the aromatic rings of BDC^{2-} of the host (the shortest C···C distances, 3.478(12) and 3.658(13) Å; dihedral angles, 15.3(4) and 73.2(3)°). The hydroxyl groups of the DHB guests are hydrogen-bonded with *sec*-amine nitrogen of the macrocycle in the host (Table 3). The 2D host layers extend parallel to the (201) plane and they are stacked in the ABCABC… manner with a slipped style, which cross-sections the brick-wall 1D channels into three (Fig. 2c). There is no open space on the side of the packed layers because the layers are packed closely by the interlayer interactions (Fig. 2d). Between the layers, π–π interactions exist between the xylyl group of the macrocycle of a layer and the BDC^{2-} rings of the adjacent layers (the shortest C···C distance, 3.571(12) Å; dihedral angle, 41.8(6)°). DHB molecules are linked to one another by the edge-to-face π–π interactions (the shortest C···C distance, 3.857(11) Å; dihedral angle, 86.1(4)°), which generates a 1D column of DHB extending along the *a* direction that passes through the channel of the network (Fig. 2e). The guest water molecules form hydrogen bonds with the uncoordinated oxygen atom of BDC^{2-} and oxygen atoms of DHB (Table 3). However, they do not interact with each other.

When **2** contains DHB guest and solvent molecules, it has no void space. However, upon removal of water and DHB guest molecules, the void volume in a unit cell estimated by PLATON[15] is 981.0 Å^3 (32.2%). TGA data for the crystalline sample **2** indicate 5.8% weight loss at 90–110 °C, which corresponds to the loss of four water guest molecules (calcd, 5.8%), and an additional 18.5% of weight loss at 215–235 °C, which corresponds to the loss of two DHB guests per formula unit (calcd, 17.6%) (Fig. S2†).

Compared with the structure of **1**, the structure of **2** is significantly changed because of the inclusion of the DHB molecules. The Cu^{II} ions show less strong tetragonal distortion than in **1**,

Table 3 The geometric parameters for the hydrogen bonding in **1–4**

Compound	D–H···A[a]	H···A/Å	D···A/Å	D–H···A/°	Symmetry code
1	N2–H2···O2	2.10	2.940(4)	154	
	N3–H3···O1W	2.10	2.969(4)	167	$x-1, y, z$
	N4–H4···O4	2.10	2.966(4)	169	$x-1, -y+1/2, z-1/2$
	N5–H5···O2W	2.10	2.986(4)	173	
	O1W–H···O1[b]	n/a	2.814(4)	n/a	
	O2W–H···O3[b]	n/a	2.698(4)	n/a	$x, -y-1/2, z+1/2$
2	N3–H3···O6	2.34	3.005(8)	130	$-x, y+1/2, -z-1/2$
	N4–H4···O2	2.13	3.003(7)	160	$x-1, -y-1/2, z-1/2$
	N5–H5···O5	2.22	3.040(8)	149	$-x+1, y-1/2, -z-1/2$
	O1W–H···O2[b]	n/a	2.802(7)	n/a	$-x+1, -y-1, -z$
	O1W–H···O4[b]	n/a	2.760(8)	n/a	$-x+1, y-1/2, -z-1/2$
	O1W–H···O5[b]	n/a	2.700(8)	n/a	$-x+1, y-1/2, -z-1/2$
	O2W–H···O2[b]	n/a	2.773(8)	n/a	$x, -y-1/2, z-1/2$
	O2W–H···O4[b]	n/a	2.792(8)	n/a	
	O2W–H···O6[b]	n/a	2.698(8)	n/a	$x+1, y, z$
3	N2–H2···O4	2.14	2.980(4)	154	$x+1, y-1, z$
	N4–H4···O2	2.10	2.954(4)	155	
	O6–H6···O2	2.03	2.625(5)	129	$-x+1, -y+1, -z$
	O1W–H···O4[b]	n/a	2.586(5)	n/a	$x+1, y, z$
	O1W–H···O4[b]	n/a	2.713(10)	n/a	$-x, -y+2, -z+1$
	O1W–H···O1W[b]	n/a	2.841(15)	n/a	$-x+1, -y+2, -z+1$
	O1W–H···O2W[b]	n/a	2.437(2)	n/a	
4	N2–H2···O3	2.13	3.007(5)	163	
	N5–H5···O2W	2.09	2.972(6)	164	
	O6–H6···O5	1.83	2.644(4)	172	
	O7–H7···O3	1.88	2.695(5)	170	$x, y+1, z$
	O8–H8···O3W	1.98	2.781(6)	167	$x, -y+3/2, z-1/2$
	O1W–H···O4[b]	n/a	2.716(5)	n/a	
	O1W–H···O5[b]	n/a	2.803(4)	n/a	$-x, y-1/2, -z+1/2$
	O1W–H···O3W[b]	n/a	2.880(6)	n/a	$-x, y-1/2, -z+1/2$
	O2W–H···O2[b]	n/a	2.820(5)	n/a	
	O4W–H···O1[b]	n/a	2.765(5)	n/a	$x, -y+1/2, z+1/2$
	O4W–H···O4[b]	n/a	2.861(6)	n/a	
	O4W–H···O6[b]	n/a	3.053(5)	n/a	$x, y-1/2, -z+1/2$

[a] D = donor and A = acceptor. [b] H atoms of the water molecules were not located.

with average Cu–N(macrocycle) and Cu–O(BDC^{2-}) bond distances of 2.020(3) Å and 2.415(4) Å, respectively. The Cu···Cu distance linked by a BDC^{2-} is 12.073(0), which is slightly increased compared with 11.952(1) Å in **1**. Each rectangular cavity in **2** has the size of 23.2 × 12.0 $Å^2$, which is increased by *ca.* 1.4 × 0.6 $Å^2$ compared with that of **1**. The shortest Cu···Cu interlayer distance is 8.973(1) Å, which is also increased as compared with that (7.881(0) Å) of **1**.

Properties and X-ray crystal structure of $[Cu_2(C_{26}H_{52}N_{10})(BDC)_2]\cdot 4HB\cdot 4H_2O$ (3)

When aqueous solutions of **A** and sodium 1,4-benzenedicarboxylate (Na_2BDC) were mixed in the presence of hydroxybenzene (HB) guest, a 1D molecular ladder that generates 3D channels was assembled. The solid **3** is soluble in water but insoluble in common organic solvents such as MeCN, MeOH, DMF, $CHCl_3$, THF, toluene, hexane, and acetone. An ORTEP drawing of the fundamental building unit of **3** is shown in Fig. 3a. An inversion centre located at the centroid of the xylyl group in the macrocyclic complex generates the other half of the bismacrocyclic complex. In **3**, all Cu^{II} bismacrocyclic units are stacked in a parallel way, and the Cu^{II} ions are linked with BDC^{2-} ions linearly to generate a 1D ladder type structure that extends along the $[1\bar{1}0]$ direction (Fig. 3b). The molecular ladders are packed parallel to each other (Fig. 3c). Intramolecular hydrogen bonding interactions exist in a ladder between the uncoordinated carbonyl oxygen atom of BDC^{2-} and the *sec*-amines of the macrocycle to form a stable six-membered ring (Table 3). The Cu^{II} ions show tetragonal distortion with the average Cu–N(macrocycle) and Cu–O(BDC^{2-}) bond distances of 2.014(2) and 2.395(2) Å, respectively. Each cavity in the ladder is made of two BDC^{2-} and four Cu^{II} ions. The Cu···Cu distances linked by BDC^{2-} and by a macrocyclic unit are 12.0 Å and 13.5 Å, respectively. The effective void size of the cavity is 6.3 × 8.7 $Å^2$ (Fig. 3b). The open-framework creates 3D channels along the *a*, *b*, and *c* directions since 1D ladders run along the [111] direction. The channels along the *a* and *b* directions are generated in the ladders and a channel along the *c* axis is formed of the free space between the ladder structures. The channels are filled with water and HB guest molecules. Guest HB molecules are included in the cavities *via* the herringbone π–π interactions with the host *via* the phenyl rings of BDC^{2-} and the xylyl group of the macrocycle (the shortest C···C distances, 3.729(8) and 3.581(9) Å; dihedral angles, 41.0(1)° and 82.5(4)°, respectively). The hydroxyl groups of the HB guests are also hydrogen-bonded with the host *via* uncoordinated carbonyl oxygen atoms of BDC^{2-} (Table 3). The water molecules included in each channel of **3** are also hydrogen bonded with the uncoordinated carbonyl oxygen atom of BDC^{2-}. A water column is formed along the

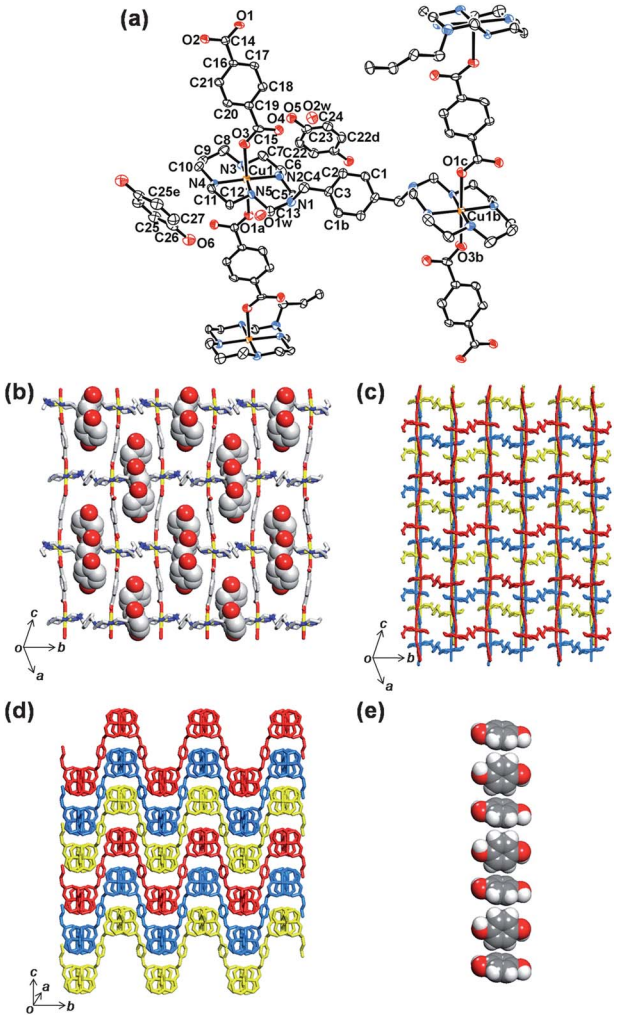

Fig. 2 The X-ray structure of **2**. (a) An ORTEP drawing with the atomic numbering scheme. The atoms are represented by 30% probable thermal ellipsoids. Symmetry operations: *a* ($x - 1$, $-y - 1/2$, $z - 1/2$), *b* ($-x + 1$, $-y - 1$, $-z - 1$), *c* ($-x + 2$, $y - 1/2$, $-z - 1/2$), *d* ($-x + 1$, $-y$, $-z - 1$), and *e* ($-x$, $-y - 1$, $-z$). (b) Top view of a 2D layer of **2**, showing the brick-wall motif cavity and DHB guests. (c) The stacking mode of 2D layers. (d) Side view of **2**. (e) A DHB column formed by the edge-to-face π–π interactions, which extends along the *a* axis.

a direction due to the hydrogen bonding interactions between themselves (Fig. 3d).

When **3** contains water and HB guest molecules, it has no void space. However, upon their removal, the void volume in a unit cell estimated by PLATON[15] becomes 790.2 Å^3 (45.7%). TGA data for the crystalline sample **3** indicate 5.2% weight loss at 25–90 °C, corresponding to the loss of four water guest molecules (calcd, 5.1%), and an additional 24.8% weight loss at 160–220 °C, which corresponds to the loss of four HB guests (calcd, 26.7%) per formula unit (Fig. S3†).

Properties and X-ray crystal structure of $[Cu_2(C_{26}H_{52}N_{10})(BDC)(H_2O)_2]\cdot(2THB\text{-}BDC)\cdot 8H_2O$ (4)

By mixing aqueous solutions of **A** and sodium 1,4-benzenedicarboxylate (Na_2BDC) in the presence of 1,3,5-trihydroxybenzene (THB), a hybrid material composed of the 1D

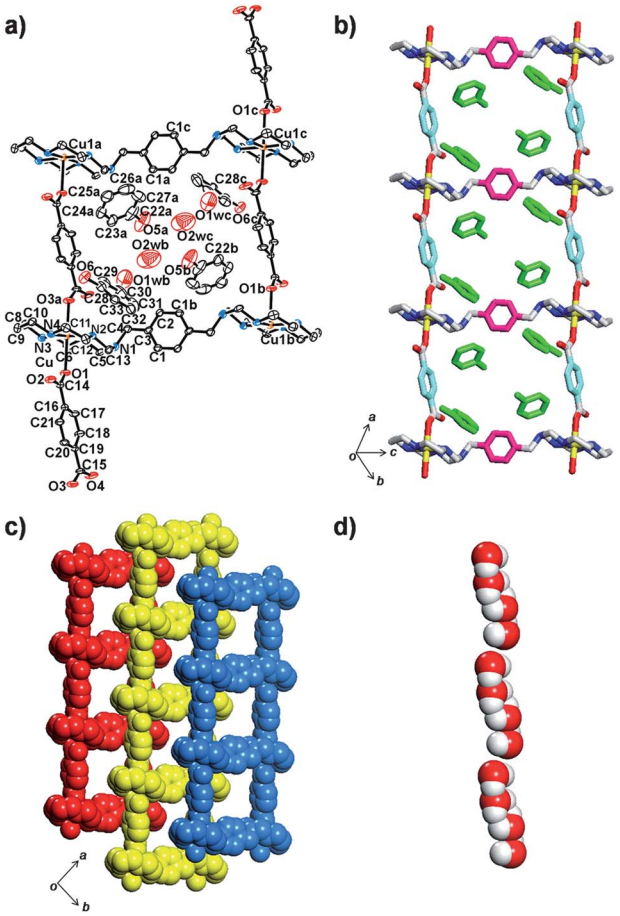

Fig. 3 The X-ray structure of **3**. (a) An ORTEP drawing with the atomic numbering scheme. The atoms are represented by 30% probable thermal ellipsoids. Symmetry operations: *a* ($x + 1$, $y - 1$, z), *b* ($-x + 1$, $-y + 1$, $-z + 1$), and *c* ($-x + 2$, $-y$, $-z + 1$). (b) The structure of a molecular ladder with HB guest molecules included in the cavity *via* π–π interactions with the host. (c) Packed structure of **3** (seen on the *ab* plane). (d) A water column formed in the channel, which extends along the *a* axis.

coordination polymer and the 2D noncovalent organic network formed of THB and BDC^{2-} (2 : 1 mol/mol ratio) was assembled. The solid **4** is soluble in water but insoluble in common organic solvents such as MeCN, MeOH, DMF, $CHCl_3$, THF, toluene, hexane, and acetone. In **4**, each Cu^{II} ion is coordinated with one BDC^{2-} ion and one water molecule at the apical position and each BDC^{2-} links two bismacrocyclic units, which generates a 1D zigzag coordination polymer chain propagating along the *c* direction (Fig. 4a). The Cu^{II} ions show a strong tetragonal distortion with average Cu–N(macrocycle) and Cu–O(H_2O and BDC^{2-}) bond distances of 2.008(2) Å and 2.642(2) Å, respectively. The bismacrocyclic complex and two guest DHB moieties lie about independent inversion centres in the unit cell: (1/2, 0, 0), (1/2, 0, 1/2), and (0, 1/2, 1/2). Two kinds of coordination polymer chains are packed in the antiparallel way to each other as shown in Fig. 4b. The shortest Cu···Cu distance between two adjacent chains is 8.976(1) Å. The 1D coordination polymer is reinforced by the H-bonding interactions between the *sec*-amine nitrogen of the macrocycle in the Cu^{II} complex and the carbonyl oxygen atom of the BDC^{2-} ion (Table 3).

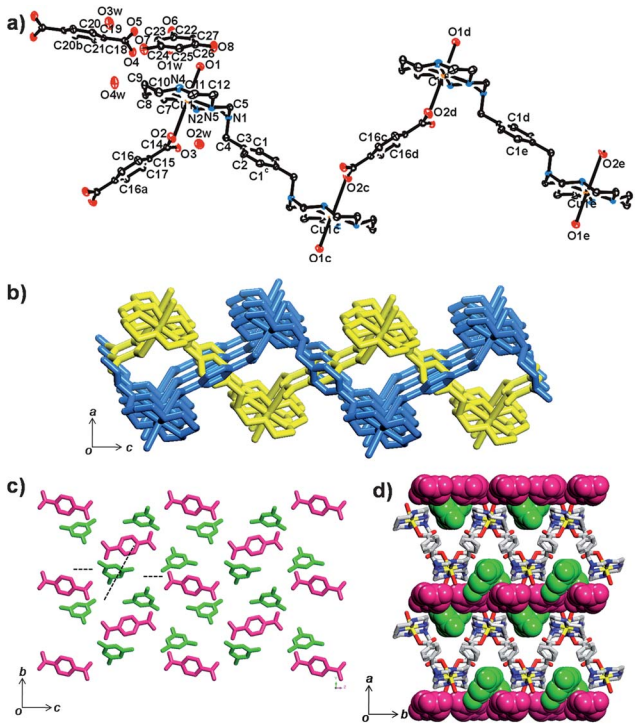

Fig. 4 The X-ray structure of **4**. (a) An ORTEP drawing of a 1D coordination polymer with atomic numbering scheme. The atoms are represented by 30% probable thermal ellipsoids. Symmetry operations: *a* (−*x* + 1, −*y*, −*z* + 1), *b* (−*x*, −*y* + 1, −*z* + 1), *c* (−*x* + 1, −*y*, −*z*), *d* (*x*, *y*, *z* − 1), *e* (−*x* + 1, −*y*, −*z* − 1), *f* (*x*, *y*, *z* − 2), and *g* (−*x* + 1, −*y*, −*z* − 2). (b) Top view of one of the host layers, which is formed of two coordination polymer chains packed in the antiparallel way to each other. (c) A view of a 2D noncovalent organic layer formed of THB molecules and BDC^{2-} linked by the π–π and H-bonding interactions. (d) Side view of **4**, showing that host coordination polymer layers (ball and stick view) and organic layers of 2THB-BDC (CPK view) are alternately packed.

As the guest molecules, two THB and one BDC^{2-} molecules are included in addition to eight H_2O molecules. Two guest THB molecules and a BDC^{2-} guest ion involving O4 are linked with each other by the herringbone π–π interactions (the shortest C···C distance, 3.679(6) Å; dihedral angle, 74.2(2)°) and the hydroxyl groups of THB are hydrogen-bonded with the BDC^{2-}, which generates a 2D noncovalent organic layer (Fig. 4c). The guest water molecules form hydrogen bonds with BDC^{2-}, THB, *sec*-amine of macrocycle, and other guest water molecules (Table 3). There exist hydrogen bonding interactions between the BDC^{2-} units of the coordination polymer chain and the THB units of the organic 2D layer, and thus the BDC^{2-} in the coordination polymer chain acts as pillars to link the organic layers together, which generates a 3D organic network (Fig. 4d).

When **4** contains guest and solvent molecules, it has no void space. However, upon removal of all guest molecules including the organic network formed of 2(THB)-(BDC^{2-}), the void volume in a unit cell estimated by PLATON[15] becomes 1508 $Å^3$ (46.7%). TGA data for the crystalline sample **4** indicate 9.6% weight loss at 25–60 °C, corresponding to the loss of eight guest water molecules (calcd, 10.3%), and an additional 31.1% weight loss at 225–275 °C, corresponding to the loss of two coordinated water and organic network formed of 2(THB)-(BDC^{2-}) per formula unit (calcd, 32.5%), which accompanies the framework decomposition (Fig. S4†).

Conclusions

The self-assembly of Cu^{II} bismacrocyclic complex (**A**) and BDC^{2-} in water results in the coordination polymer networks with brick-wall, ladder, and chain structures, depending on the type of templating guest molecules such as H_2O, HB, DHB, and THB. The host structures are stabilized by the guest molecules *via* the hydrogen bonding or π–π stacking interactions, and the guest molecules are assembled to a 1D column or a 2D layer, being affected by the host structures. The results reveal that the host structures and assembly of guest molecules are mutually dependent. These suggest that the host structure can be easily modulated by changing the template guest molecule.

Experimental section

General methods

All chemicals and solvents used in the syntheses were of reagent grade and used without further purification. Infrared spectra were recorded with a Perkin Elmer 2000 FT-IR spectrophotometer. Elemental analyses were performed by the National Center for Inter-University Research Facilities in Seoul National University. UV/Vis spectra were recorded on a Cary 300 Bio UV/Vis spectrophotometer. Thermogravimetric analysis (TGA) was performed under N_2 at a scan rate of 5 °C min^{-1} using a 2050 Thermogravimetric Analyzer, TA Instruments. Differential Scanning Calorimetry (DSC) was performed under N_2 at a scan rate of 10 °C min^{-1} using a 2010 Differential Scanning Calorimeter, TA Instruments.

Preparation of $[Cu_2(C_{26}H_{52}N_{10})(Cl)_4]\cdot 6H_2O$ (A)

To a stirred methanol solution (180 mL) of $CuCl_2\cdot 2H_2O$ (3.42 g, 0.0201 mol), were slowly added *N*,*N*′-bis(2-aminoethyl)-1,3-propanediamine (3.30 g, 0.0200 mol), *p*-xylylenediamine (1.38 g, 0.0101 mol), and paraformaldehyde (2.55 g, 0.0849 mol). The mixture was heated at reflux for 5 days. The solution was allowed to stand at room temperature for 1–2 h. Purple precipitate formed, which was filtered off, washed with methanol, and dried in air. The crude purple precipitate was recrystallized in the hot mixture of water and methanol (3 : 1, v/v). Yield: 42%; elemental analysis calcd (%) for $Cu_2C_{26}H_{64}N_{10}Cl_4O_6$ (fw 881.75): C 35.41, H 7.32, N 15.88; found: C 35.71, H 6.00, N 15.77; FT-IR (Nujol): ν = 3344 (s, br), 3250 (s), 3166 (s), 1106 (m), 1065 (s), 1015 (s), 1000 (s), 721 (w) cm^{-1}; UV/Vis (H_2O): λ_{max} (ε) = 506 nm (185 M^{-1} cm^{-1}).

Preparation of $[Cu_2(C_{26}H_{52}N_{10})(BDC)_2]\cdot 4H_2O$ (1)

An aqueous solution (1.5 mL) of Na_2BDC (0.063 g, 0.30 mmol) was dropwise added to an aqueous solution (3 mL) of **A** (0.088 g, 0.10 mmol). To the resulting red solution, was added DMF (5 mL). The mixture was allowed to stand at room temperature until pale purple crystals formed, which were filtered off, washed with water, and dried in air. Yield: 80%; elemental analysis calcd (%) for $Cu_2C_{42}H_{68}N_{10}O_{12}$ (fw 1032.14): C 48.87, H 6.64, N 13.57;

found: C 49.45, H 6.68, N 13.84; FT-IR (Nujol): $\nu = 3316$ (s, br), 3142 (s), 1621 (m), 1567 (s), 1558 (s), 1338 (s) cm^{-1}; UV/Vis (diffuse reflectance spectrum): $\lambda_{max} = 514$ nm.

Preparation of $[Cu_2(C_{26}H_{52}N_{10})(BDC)_2]\cdot 2DHB\cdot 4H_2O$ (2)

A (0.088 g, 0.10 mmol) was dissolved in the aqueous solution (4 mL) of 1,4-dihydroxybenzene (0.056 g, 0.51 mmol), and then the aqueous solution (2 mL) of Na_2BDC (0.063 g, 0.30 mmol) was added dropwise. The mixture was allowed to stand at room temperature until deep purple crystals formed, which were filtered off, washed with aqueous solution (2 mL) of 1,4-dihydroxybenzene (0.028 g), and dried in air. Yield: 82%; elemental analysis calcd (%) for $Cu_2C_{54}H_{80}N_{10}O_{16}$ (fw 1252.36): C 51.79, H 6.44, N 11.18; found: C 52.10, H 6.50, N 11.34; FT-IR (Nujol): $\nu = 3270$ (s), 3227 (s), 3132 (s), 1668 (w), 1568 (s), 1520 (m), 1348 (s) cm^{-1}; UV/Vis (diffuse reflectance spectrum): $\lambda_{max} = 540$ nm.

Preparation of $[Cu_2(C_{26}H_{52}N_{10})(BDC)_2]\cdot 4HB\cdot 4H_2O$ (3)

A (0.088 g, 0.10 mmol) was dissolved in the aqueous solution (4 mL) of hydroxybenzene (0.063 g, 0.67 mmol). Then the aqueous solution (2 mL) of Na_2BDC (0.063 g, 0.30 mmol) was added dropwise. The mixture was allowed to stand at room temperature until purple crystals formed, which were filtered off, washed with aqueous solution (2 mL) of hydroxybenzene (0.032 g), and dried in air. Yield: 89%; elemental analysis calcd (%) for $Cu_2C_{66}H_{92}N_{10}O_{16}$ (fw 1408.58): C 56.28, H 6.58, N 9.94; found: C 56.32, H 6.44, N 9.82; FT-IR (Nujol): $\nu = 3267$ (m), 3247 (s), 3114 (s), 1568 (s), 1558 (s), 1498 (w), 1274 (m) cm^{-1}; UV/Vis (diffuse reflectance spectrum): $\lambda_{max} = 543$ nm.

Preparation of $[Cu_2(C_{26}H_{52}N_{10})(BDC)(H_2O)_2]\cdot(2THB\text{-}BDC)\cdot 8H_2O$ (4)

A (0.088 g, 0.10 mmol) was dissolved in the aqueous solution (4 mL) of 1,3,5-trihydroxybenzene dihydrate (0.054 g, 0.33 mmol), and then the aqueous solution (2 mL) of Na_2BDC (0.063 g, 0.30 mmol) was added dropwise. The mixture was allowed to stand at room temperature until pale purple crystals formed, which were filtered off, washed with aqueous solution (2 mL) of 1,3,5-trihydroxybenzene dihydrate (0.027 g), and dried in air. Yield: 91%; elemental analysis calcd (%) for $Cu_2C_{54}H_{92}N_{10}O_{24}$ (fw 1392.46): C 46.58, H 6.66, N 10.06; found: C 46.40, H 6.65, N 9.96; FT-IR (Nujol): $\nu = 3231$ (m), 3131 (m), 1621 (m), 1558 (s), 1505 (s), 1329 (m) cm^{-1}; UV/Vis (diffuse reflectance spectrum): $\lambda_{max} = 505$ nm.

X-Ray crystallography

Diffraction data for **1–4** were collected with an Enraf-Nonius Kappa CCD diffractometer (MoKα, $\lambda = 0.71073$ Å, graphite monochromator). Preliminary orientation matrices and unit cell parameters were obtained from the peaks of the first ten frames and were then refined using the whole dataset. Frames were integrated and corrected for Lorentz and polarization effects using DENZO.[17] The scaling and the global refinement of crystal parameters were performed by SCALEPACK.[17] No absorption correction was made. The crystal structures were solved by the direct methods[18] and refined by full-matrix least-squares refinement using the SHELXL-97 computer program.[19] The positions of all non-hydrogen atoms were refined with anisotropic displacement factors. The hydrogen atoms were positioned geometrically by using a riding model. The crystallographic data of **1–4** are summarized in Table 1. The crystal structures are compared in Table 2. Details of hydrogen bondings in the crystal structures are given in Table 3.† Crystallographic data for the structures reported in this paper have been deposited with the Cambridge Crystallographic Data Centre as supplementary publication nos. CCDC-747625 (1), CCDC-747626 (2), CCDC-747627 (3), and CCDC-747628 (4). These data can be obtained free of charge from The Cambridge Crystallographic Data Centre via www.ccdc.cam.ac.uk/data_request/cif.

Acknowledgements

This work was supported by National Research Foundation of Korea (NRF) Grant funded by the Korean Government (MEST) (no. 2011-0031432 and no. 2011-0001341). H. J. Park acknowledges a support from Seoul Science Fellowship.

References

1 (*a*) E. Y. Lee, S. Y. Jang and M. P. Suh, *J. Am. Chem. Soc.*, 2005, **127**, 6374–6381; (*b*) H.-S. Choi and M. P. Suh, *Angew. Chem., Int. Ed.*, 2009, **48**, 6865–6869; (*c*) H. J. Park, Y. E. Cheon and M. P. Suh, *Chem.–Eur. J.*, 2010, **16**, 11662–11669; (*d*) T. K. Prasad, D. H. Hong and M. P. Suh, *Chem.–Eur. J.*, 2010, **16**, 14043–14050.

2 (*a*) H. J. Choi and M. P. Suh, *J. Am. Chem. Soc.*, 2004, **126**, 15844–15851; (*b*) M. P. Suh, J. W. Ko and H. J. Choi, *J. Am. Chem. Soc.*, 2002, **124**, 10976–10977.

3 (*a*) H. R. Moon, J. H. Kim and M. P. Suh, *Angew. Chem., Int. Ed.*, 2005, **44**, 1261–1265; (*b*) E. Y. Lee and M. P. Suh, *Angew. Chem., Int. Ed.*, 2004, **43**, 2798–2801; (*c*) J. W. Ko, K. S. Min and M. P. Suh, *Inorg. Chem.*, 2002, **41**, 2151–2157; (*d*) H. J. Choi, T. S. Lee and M. P. Suh, *Angew. Chem., Int. Ed.*, 1999, **38**, 1405–1408; (*e*) H. J. Choi and M. P. Suh, *J. Am. Chem. Soc.*, 1998, **120**, 10622–10628.

4 (*a*) B. Chen, C. Liang, J. Yang, D. S. Contreras, Y. L. Clancy, E. B. Lobkovsky, O. M. Yaghi and S. Dai, *Angew. Chem., Int. Ed.*, 2006, **45**, 1390–1393; (*b*) K. S. Min and M. P. Suh, *Chem.–Eur. J.*, 2001, **7**, 303–313; (*c*) H. J. Choi, T. S. Lee and M. P. Suh, *J. Inclusion Phenom. Macrocyclic Chem.*, 2001, **41**, 155–162.

5 (*a*) H. J. Park and M. P. Suh, *Chem. Commun.*, 2010, **46**, 610–612; (*b*) H. J. Park and M. P. Suh, *Chem.–Eur. J.*, 2008, **14**, 8812–8821; (*c*) Y.-G. Lee, H. R. Moon, Y. E. Cheon and M. P. Suh, *Angew. Chem., Int. Ed.*, 2008, **47**, 7741–7745; (*d*) M. Dincă and J. R. Long, *Angew. Chem., Int. Ed.*, 2008, **47**, 6766–6779; (*e*) S. S. Kaye, A. Dailly, O. M. Yaghi and J. R. Long, *J. Am. Chem. Soc.*, 2007, **129**, 14176–14177; (*f*) H. Furukawa, M. A. Miller and O. M. Yaghi, *J. Mater. Chem.*, 2007, **17**, 3197–3204; (*g*) M. Dincă, A. Dailly, Y. Liu, C. M. Brown, D. A. Neumann and J. R. Long, *J. Am. Chem. Soc.*, 2006, **128**, 16876–16883; (*h*) A. R. Millward and O. M. Yaghi, *J. Am. Chem. Soc.*, 2005, **127**, 17998–17999; (*i*) S. Ma, D. Sun, J. M. Simmons, C. D. Collier, D. Yuan and H.-C. Zhou, *J. Am. Chem. Soc.*, 2008, **130**, 1012–1016.

6 (*a*) J.-R. Li, R. J. Kuppler and H.-C. Zhou, *Chem. Soc. Rev.*, 2009, **38**, 1477–1504; (*b*) Q. Li, W. Zhang, O. Š. Miljanić, C.-H. Sue, Y.-L. Zhao, L. Liu, C. B. Knobler, J. F. Stoddart and O. M. Yaghi, *Science*, 2009, **325**, 855–859; (*c*) Y. E. Cheon, J. Park and M. P. Suh, *Chem. Commun.*, 2009, 5436–5438; (*d*) T. K. Maji, R. Matsuda and S. Kitagawa, *Nat. Mater.*, 2007, **6**, 142–148; (*e*) Y. E. Cheon and M. P. Suh, *Chem.–Eur. J.*, 2008, **14**, 3961–3967; (*f*) S. Ma, D. Sun, X.-S. Wang and H.-C. Zhou, *Angew. Chem., Int. Ed.*, 2007, **46**, 2458–2462.

7 (*a*) K. S. Min and M. P. Suh, *J. Am. Chem. Soc.*, 2000, **122**, 6834–6840; (*b*) H. J. Choi and M. P. Suh, *Inorg. Chem.*, 2003, **42**, 1151–1157; (*c*) Y. Liu, G. Li, X. Li and Y. Cui, *Angew. Chem., Int. Ed.*, 2007, **46**, 6301–6304.

8 (*a*) Y. E. Cheon and M. P. Suh, *Angew. Chem., Int. Ed.*, 2009, **48**, 2899–2903; (*b*) F. Schröder, D. Esken, M. Cokoja, M. W. E. van den Berg, O. I. Lebedev, G. Van Tendeloo, B. Walaszek, G. Buntkowsky, H.-H. Limbach, B. Chaudret and R. A. Fischer, *J. Am. Chem. Soc.*, 2008, **130**, 6119–6130; (*c*) M. P. Suh, H. R. Moon, E. Y. Lee and S. Y. Jang, *J. Am. Chem. Soc.*, 2006, **128**, 4710–4718.

9 (*a*) B. Chen, L. Wang, F. Zapata, G. Qian and E. B. Lobkovsky, *J. Am. Chem. Soc.*, 2008, **130**, 6718–6719; (*b*) C. A. Bauer, T. V. Timofeeva, T. B. Settersten, B. D. Patterson, V. H. Liu, B. A. Simmons and M. D. Allendorf, *J. Am. Chem. Soc.*, 2007, **129**, 7136–7144; (*c*) S. Shimomura, R. Matsuda, T. Tsujino, T. Kawamura and S. Kitagawa, *J. Am. Chem. Soc.*, 2006, **128**, 16416–16417.

10 (*a*) C. Serre, C. Mellot-Draznieks, S. Surble, N. Audebrand, Y. Filinchuk and G. Férey, *Science*, 2007, **315**, 1828–1831; (*b*) G. J. Halder and C. J. Kepert, *J. Am. Chem. Soc.*, 2005, **127**, 7891–7900; (*c*) Y. Zhang, B. Chen, F. R. Fronczek and A. W. Maverick, *Inorg. Chem.*, 2008, **47**, 4433–4435; (*d*) O. Ohmori, M. Kawano and M. Fujita, *Angew. Chem., Int. Ed.*, 2005, **44**, 1962–1964; (*e*) D. N. Dybtsev, H. Chun and K. Kim, *Angew. Chem., Int. Ed.*, 2004, **43**, 5033–5036; (*f*) S. R. Halper, L. Do, J. R. Stork and S. M. Cohen, *J. Am. Chem. Soc.*, 2006, **128**, 15255–15268.

11 (*a*) S. M. Nevilee, B. Mouvaraki, K. Murray and C. J. Kepert, *Angew. Chem., Int. Ed.*, 2007, **46**, 2059–2062; (*b*) S. Libri, M. Mahler, G. M. Espallargas, D. C. N. G. Singh, J. Soleimannejad, H. Adams, M. D. Burgard, N. P. Rath, M. Brunelli and L. Brammer, *Angew. Chem., Int. Ed.*, 2008, **47**, 1693–1697; (*c*) S. K. Ghosh, S. Bureekaew and S. Kitagawa, *Angew. Chem., Int. Ed.*, 2008, **47**, 3403–3406; (*d*) E. Deiters, V. Bulach and M. W. Hosseini, *Chem. Commun.*, 2005, 3906–3908; (*e*) T. Kawamichi, T. Kodama, M. Kawano and M. Fujita, *Angew. Chem., Int. Ed.*, 2008, **47**, 8030–8032; (*f*) C.-D. Wu and W. Lin, *Angew. Chem., Int. Ed.*, 2005, **44**, 1958–1961.

12 C. B. Aakeröy, N. R. Champness and C. Janiak, *CrystEngComm*, 2010, **12**, 22–43.

13 M. P. Suh, *Adv. Inorg. Chem.*, 1997, **44**, 93–146.

14 M. P. Suh and S. K. Kim, *Inorg. Chem.*, 1993, **32**, 3562–3564.

15 A. L. Spek, *PLATON A Multipurpose Crystallographic Tool*, Utrecht University, Utrecht, The Netherlands, 2007.

16 The gas sorption study was carried out on **1** after removing the guests by heating it to 100 °C at 10^{-5} Torr for 4 h.

17 Z. Otwinowsky and W. Minor, *Processing of X-Ray Diffraction Data Collected in Oscillation Mode, Methods in Enzymology*, ed. C. W. Carter and R. M. Sweet, Academic Press, 1996, vol. 276, pp. 307–326.

18 G. M. Sheldrick, *Acta Crystallogr., Sect. A: Fundam. Crystallogr.*, 1990, **46**, 467.

19 G. M. Sheldrick, *SHELXL97. Program for the Crystal Structure Refinement*, University of Göettingen, Göettingen, Germany, 1997.